

A Parametric Analysis on the Influence of the Binder Characteristics on the Behaviour of Passive Rock Bolts with the Block Reinforcement Procedure

Original

A Parametric Analysis on the Influence of the Binder Characteristics on the Behaviour of Passive Rock Bolts with the Block Reinforcement Procedure / Oreste, P.; Spagnoli, G.; Buccoleri, A. G.. - In: GEOTECHNICAL AND GEOLOGICAL ENGINEERING. - ISSN 0960-3182. - STAMPA. - 38:4(2020), pp. 4159-4168. [[10.1007/s10706-020-01285-7](https://doi.org/10.1007/s10706-020-01285-7)]

Availability:

This version is available at: 11583/2940994 since: 2021-11-28T20:40:11Z

Publisher:

Springer

Published

DOI:[10.1007/s10706-020-01285-7](https://doi.org/10.1007/s10706-020-01285-7)

Terms of use:

This article is made available under terms and conditions as specified in the corresponding bibliographic description in the repository

Publisher copyright

(Article begins on next page)

1 **A parametric analysis on the influence of the binder characteristics on the behav-**
2 **our of passive rock bolts with the Block Reinforcement Procedure**

3 Pierpaolo Oreste¹, Giovanni Spagnoli^{2*}, Andrea Giuseppe Buccoleri³,

4 ¹ Department of Environmental, Land and Infrastructure Engineering, Politecnico di Torino,
5 Corso Duca Degli Abruzzi 24, 10129 Torino, Italy, pierpaolo.oreste@polito.it ORCID:

6 0000-0001-8227-9807

7 ² BASF Construction Solutions GmbH, Dr-Albert-Frank-Strasse 32, 83308 Trostberg, Ger-
8 many, *corresponding author, Tel: +49 8621 86-3702, giovanni.spagnoli@basf.com OR-

9 CID: 0000-0002-1866-4345

10 ³ Department of Environmental, Land and Infrastructure Engineering, Politecnico di Torino,
11 Corso Duca Degli Abruzzi 24, 10129 Torino, Italy, [andreagiuseppe.buccoleri@stu-](mailto:andreagiuseppe.buccoleri@studenti.polito.it)

12 [denti.polito.it](mailto:andreagiuseppe.buccoleri@studenti.polito.it)

13 **Abstract**

14 An extensive parametric analysis of 729 typical cases was developed with a calculation pro-
15 cedure allowing to simulate in detail the behavior of the passive bolts and their interaction
16 with the surrounding rock. The parametric analysis allowed to evaluate the effectiveness of
17 the bolts, on the basis of the extent of the stabilization forces produced, in relation to the
18 geometric and mechanical characteristics of the binder used in the realization of the bolts.
19 Different bolt diameters and lengths, binder thickness and elastic moduli and block displace-
20 ment with respect to the horizontal plane have been considered. It has been possible to
21 detect how such parameters have a great influence on the mechanical behavior of the bolt
22 and on the extent of the stabilizing forces which are applied to the potentially unstable rock
23 block. For this reason, therefore, the definition of the characteristics of the binder (and in

24 particular the thickness of the binder around the steel bar and the elastic modulus of the
25 binder itself) cannot be assessed only in relation to application aspects, but it must be able
26 to consider the effects on the efficiency of the bolt and in particular on the stabilization forces
27 on the potentially unstable rock block.

28 **Key words:** rock bolt; rock; binder; elastic modulus; Block Reinforcement Procedure; para-
29 metric analysis, rock-bolt interaction

30

31 **Abbreviations and nomenclature**

32 BRP Block reinforcement procedure

33 CMC Continuously mechanically coupled

34 DEFE Doubly enriched finite element

35 LEM Limit equilibrium method

36 UCS Unconfined compressive strength

37 FS Factor of safety

38 EA Axial stiffness of the bolt

39 E_{binder} Elastic modulus of the binder surrounding the steel bar in the hole

40 $E_{binder, \infty}$ Elastic modulus for the cementitious grout for a time, t , very large;

41 EJ Bending stiffness of the bolt

42 E_{st} Steel elastic modulus

43 i Intersecting line of the sliding surfaces, coinciding with the direction of the block dis-
44 placement vector

45 k Link between the transverse displacements, y , of the bolt and the normal pressure,
46 p , which is applied on the perimeter of the bolt (on the wall of the hole) by the surrounding
47 rock

48 L_a Length of each single bolt inside the unstable block

49 L_p Bolt length in the stable rock behind the unstable one

50 M Bending moments

51 N Axial forces

52 N_0 Value of the tensile stress applied in the axial direction of the bolt

- 53 p Value of the normal pressure which is applied on the perimeter of the bolt
- 54 P_{hole} Perimeter of the cross-section of the bolt
- 55 T Shear forces
- 56 t Time
- 57 t_{binder} Thickness of the binder annulus surrounding the bar
- 58 T_0 Value of the shear stress applied
- 59 v_r Value of the relative axial displacement of the bolt-rock
- 60 y Transversal displacements of the bolt
- 61 α Parameter characterizing the interaction in the axial direction between bolt and rock
- 62 $\alpha = \sqrt{\frac{\beta_c \cdot P_{hole}}{EA}}$
- 63 β Parameter that characterizes the interaction in the transverse direction between bolt
- 64 and rock $\beta = \sqrt[4]{\frac{k \cdot \Phi_{hole}}{4 \cdot EJ}}$
- 65 β_c Link between the relative axial displacements, v_r , and the shear stresses, τ , that de-
- 66 velop on the perimeter of the bolt
- 67 δ Arbitrary displacement to the block
- 68 δ_{max} Maximum displacement of the block which the bolt system can support
- 69 δ_n Displacement in the axial direction of the bolt
- 70 δ_t Displacement in the transversal direction of the bolt
- 71 ε_E Constant (inverse dimension of time) indicating the rate with which the elastic modulus
- 72 evolves from the initial null value to the asymptotic value $E_{grout, \infty}$
- 73 γ_{displ} Angle of the block with respect to the horizontal plane

- 74 η_{min} Minimum ratio between each local safety factor divided by the respective minimum
- 75 permissible value required
- 76 σ_{yield} Steel yield stress
- 77 τ_{lim} Limit shear stress at the bolt-rock interface
- 78 ν_{binder} Poisson coefficient of the binder
- 79 Φ_{hole} Diameter of the hole
- 80 Φ_{bar} Bolt (bar) diameter
- 81 ψ_{bolt} Bolt inclination with the horizontal plane
- 82

83 Introduction

84 In order to control and prevent both major and local instabilities of the rock mass during
85 underground, different support systems such as meshing, sprayed concrete and anchoring
86 are used (e.g. Chen, 2004; Oreste, 2008; Oreste, 2013). Fully grouted bolts are used for
87 instance to prevent rock blocks from falling in fractured rocks in order to 'lock together' blocks
88 in heavily jointed rock masses to create a "reinforced arch" around an underground opening
89 that is capable of providing stability to the cavity (Lang, 1961).

90 A fully grouted bolt intersected by a joint could influence the shearing of a joint increasing
91 the bolt resistance due to an increase in axial, shear forces and bending moments in the
92 bolt rod (Das et al., 2013; Oreste and Dias 2012; Ranjbarnia et al., 2014; 2016).

93 Rock bolting not only strengthens or stabilizes a jointed rock mass, but also has a marked
94 effect on the rock mass stiffness (Chappell, 1989). Furthermore, where the *in situ* rock
95 stresses increase, rock support is used to prevent the failed rock from disintegration (Li,
96 2017).

97 Rock bolts are widely used to reinforce the rock mass and stabilize jointed surrounding rock,
98 because of their ease of installation, versatility and relatively low cost of rebars in compari-
99 son to their alternative counterparts (Indraratna and Kaiser, 1990). Passive reinforcing ele-
100 ments have a zero initial load and the mobilized stabilizing load increases with the displace-
101 ment of the potentially unstable rock block. However, also active bolts can be used, which
102 assure overall stability and provide confinement to the rock mass between the two ends of
103 the element, as the tensile load transfers from the element as an active compressive load
104 to the rock mass increasing the resulting stress confinement in the rock (Carranza-Torres,
105 2009; He et al., 2015).

106 Rock bolts generally consist of steel rods with a mechanical or chemical anchor at one end
107 and a face plate and nut at the other (Bawden, 2011). Continuously mechanically coupled

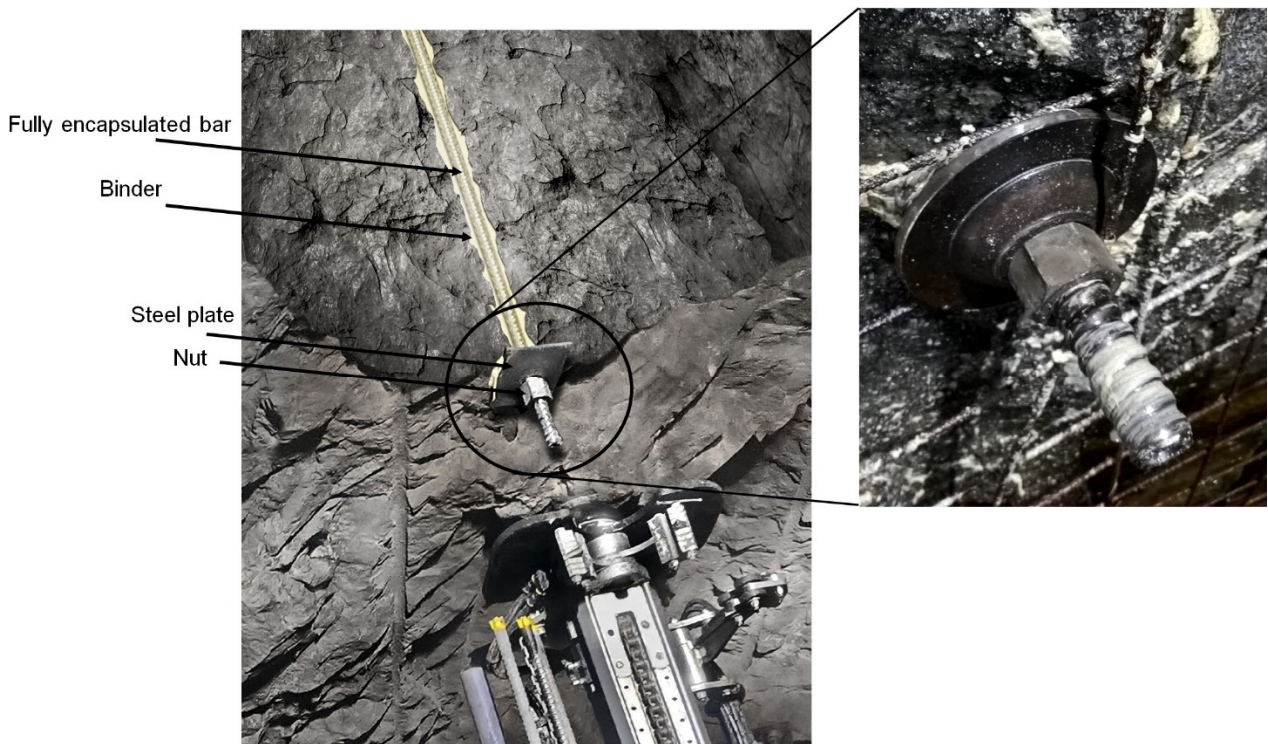
108 (CMC) bolts rely on a binder that fills the annulus between the element and the borehole
109 wall (see Fig. 1).

110 The load transfer through the bond between the element and the rock causes tension in the
111 bolt. As a result of the rock bolt deformation, the relative shear force will act on the rock
112 mass and restrain the further deformation of the rock, transferring load from the stable ex-
113 terior to the interior of the rock mass (Nie et al. 2014).

114 Rock bolts are also used for the stabilization of potentially unstable blocks due to sliding
115 from the walls of rocky excavation fronts on the surface or from side walls of underground
116 works. This type of bolts operates by applying to the potentially unstable blocks two direct
117 forces, the first one, along the axis of the bolt and the second one, perpendicular to the first
118 one and having a direction that depends on the vector displacement of the block (Oreste
119 and Cravero, 2008). Passive bolts are loaded and transmit stabilizing forces with the move-
120 ments of the rock mass and in particular with the displacement of the potential unstable
121 block. At the time of their installation they have a zero initial load which increases until the
122 block is completely stabilized. The role of the interface with the rock is fundamental for the
123 functioning of the bolt. The physical and mechanical characteristics of the cementitious (or
124 resin) binders are, therefore, decisive, but often neglected in the design phase of the bolt
125 installation procedure.

126 In this paper a simplified calculation method the Block Reinforcement Procedure (BRP)
127 (Oreste and Cravero, 2008; Oreste, 2009) is used for performing a parametric analysis to
128 study potentially unstable small-medium sized rock blocks on the walls of an underground
129 excavation, reinforced by passive fully grouted bolts. The procedure applies the Limit Equi-
130 librium Method (LEM) and the bolt is schematized as a beam while the bolt-rock interaction
131 considers a continuous bed of Winkler springs (Lancellota and Cavallera 1999), in both the
132 axial and transversal directions. More specifically, the parametric study aimed to analyze in
133 detail the influence of the characteristics of the bolt-rock interface on the behavior of the bolt

134 and, therefore, on its effectiveness in transmitting the stabilizing forces to the potentially
135 unstable block.



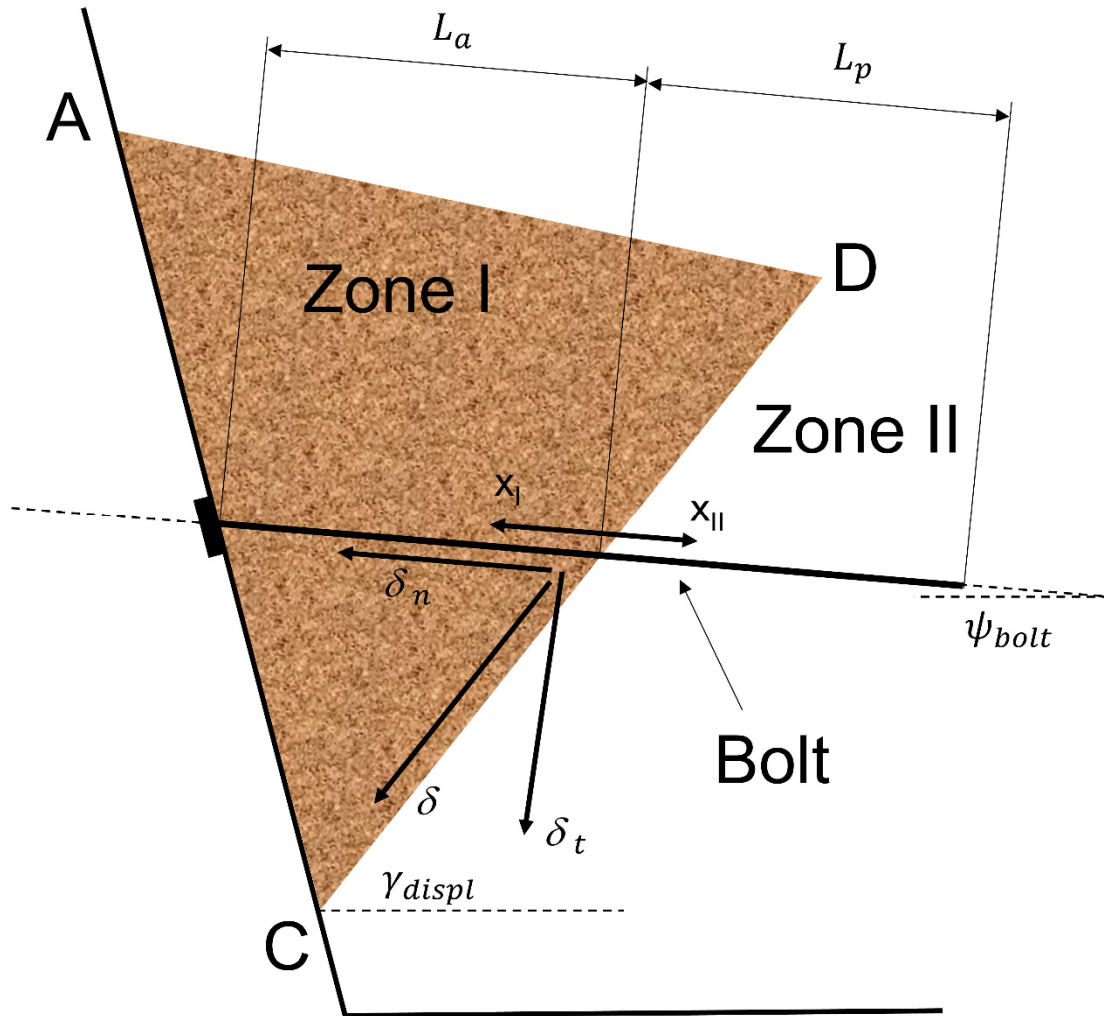
136

137 **Fig. 1 Picture a fully encapsulated rock bolt**

138 **The numerical model used for the parametric analysis**

139 The calculation model used, called BRP, was introduced by Oreste and Cravero (2008) and
140 Oreste (2009). This model maintains the simplicity typical of analytical calculation methods
141 but achieves a satisfactory precision in the analysis of the interaction between fully encap-
142 sulated passive bolt and rock, for the stabilization of rock blocks isolated by natural discon-
143 tinuities. These bolts cross the potentially unstable blocks and reach the stable rock behind
144 them, where they penetrate for a certain length (L_p) (Figure 2). Fig. 2 shows L_a , which is the
145 length of the bolt inside the unstable block (Zone I); L_p , which is the length of the remaining
146 part of the bolt in stable rock (Zone II); A, B, and D are the vertices of the rock block; δ
147 represents the displacement of the block along the sliding direction; δ_n and δ_t are respec-
148 tively the components of the displacement in the axial and normal direction; x is the axial

149 coordinate along the bolt; γ_{displ} is the angle between the sliding direction and the horizontal
150 plane; ψ_{bolt} is the inclination of the bolt with the horizontal plane.



151

152 **Fig. 2 Schematic representation (not to scale) of the potentially unstable rock block**
153 **and of the passive bolt passing through it.**

154 The method allows the evaluation of the forces (axial N and shear T) and of the bending
155 moments M developing along the bolt, as a linear function of the (very small) displacements
156 of the block. Then the stabilizing forces, applied by the single bolt to the potentially unstable
157 block, are determined. These are essentially the N and T forces that develop in the bolt at
158 the intersection with the sliding surface. The displacement of the block considered is the

159 maximum one which leads to the limit conditions of the bolts. The main phases of the cal-
160 culation are as follows (Oreste and Cravero, 2008):

161 a) definition of the geometry of the problem (number, position, orientation of the bolts
162 with respect to the block, the length of each single bolt inside the block, L_a , and the
163 bolt length in the stable rock behind the unstable one, L_p) (Figure 2);

164 b) assignment of an arbitrary displacement to the block δ , compatible with the geometry
165 and with the sliding surfaces identified; determination of the two components of the
166 displacement δ for each bolt: one in the axial direction of the bolt δ_n and the other in
167 the transverse direction δ_t (Figure 2);

168 c) on the basis of the two values of the displacement, δ_n and δ_t , the values of N , T , M
169 and the value of the relative axial displacement of the bolt-rock v_r and the relative
170 transversal displacement along the bolt are then identified;

171 d) determination of the local safety factors in the bolt and on the bolt-rock interface, in
172 order to verify the working conditions of the bolt in the presence of the arbitrary dis-
173 placement δ applied to the block;

174 e) comparison of the local safety factors obtained in the previous point with the required
175 minimum admissible values: the minimum ratio (η_{min}) between each local safety fac-
176 tor divided by the respective minimum permissible value required, among all the in-
177 stalled bolts, allows to determine the maximum displacement of the block which the
178 bolt system can admit: $\delta_{max} = \frac{\delta}{\eta_{min}}$;

179 f) re-determination of N , T , M , v_r and y in correspondence with the displacement of the
180 block equal to δ_{max} . It is interesting for the evaluation of the block stability to consider
181 the values of N and T at the intersection with the sliding surface of the block (N_0 and
182 T_0): they are also the maximum values of N and T along the bolt. The values N_0 and
183 T_0 are also the forces that each bolt applies to the potentially unstable block: N_0 is the

184 force applied in the axial direction of the bolt, T_0 is the force applied in the direction
185 of the intersection line between the transversal plane to the bolt and the plane com-
186 prising the bolt itself and the block displacement vector;

187 g) determination of the global safety factor of the block in the presence of bolting, con-
188 sidering the forces N_0 and T_0 that each bolt applies to the potentially unstable block.

189 The procedure between steps a) and g) is repeated until a configuration of the bolt system
190 is judged satisfactory with respect to the overall safety factor of the block.

191 To derive the forces N_0 and T_0 , which are applied by each bolt to the rock block, the effects
192 of the axial component and of the transversal component of the displacement of the block,
193 δ , are analyzed separately. The axial component δ_n allows to determine the axial force N
194 and the relative axial displacement v_r along the bolt, while the transverse component δ_t
195 allows to determine T , M and the transverse displacement y along the bolt.

196 More specifically, N_0 and T_0 , are determined with the following equations:

$$197 \quad N_0 = EA \cdot \alpha \cdot \left(-\frac{(1-e^{-2\alpha L_p}) \cdot e^{-2\alpha L_a}}{2 \cdot [1+e^{-2\alpha(L_a+L_p)}]} - \frac{(1-e^{-2\alpha L_p})}{2 \cdot [1+e^{-2\alpha(L_a+L_p)}]} \right) \cdot \delta_{n,max} \quad (1)$$

$$198 \quad T_0 = EJ \cdot \beta^3 \cdot \delta_{t,max} \quad (2)$$

199 where:

200 EA is the axial stiffness of the bolt;

201 EJ is the bending stiffness of the bolt;

202 L_a is the crossing bolt length in the block;

203 L_p is the bolt length in the stable rock behind the block;

204 α is a parameter characterizing the interaction in the axial direction between bolt and rock

$$205 \quad \alpha = \sqrt{\frac{\beta_c \cdot P_{hole}}{EA}};$$

206 P_{hole} is the perimeter of the cross-section of the bolt;

207 β_c is the link between the relative axial displacements, v_r , and the shear stresses, τ , that
208 develop on the perimeter of the bolt (on the wall of the hole); β_c depends in general on the
209 characteristics of the material surrounding the steel bar and on the elastic modulus of the
210 rock;

211 β is a parameter that characterizes the interaction in the transverse direction between bolt
212 and rock $\beta = \sqrt[4]{\frac{k \cdot \Phi_{hole}}{4 \cdot EJ}}$,

213 k is the link between the transverse displacements, y , of the bolt and the normal pressure,
214 p , which is applied on the perimeter of the bolt by the surrounding rock;

215 Φ_{hole} is the diameter of the hole.

216

217 Equation 2 is valid for sufficiently high values of L_a and L_p (greater than or equal to 1m).

218 The characteristics of the material that is used to connect the steel bar to the rock (usually
219 cement grout or resin, e.g. Littlejohn and Bruce 1977; Henning and Ferreira 2010) affect the
220 axial stiffness of the bolt (EA), the transverse stiffness (EJ), the parameter β_c of interaction
221 in the axial direction and the parameter k which links the trasversal displacements y to the
222 pressure p applied to the perimeter of the bolt. They prove to be very important in the func-
223 tioning mechanism of the bolt and in particular in the evaluation of the stabilization forces
224 that the bolt succeeds in transmitting to the rock block.

225 Axial and transverse stiffness can be obtained from the following expressions (Oreste and
226 Cravero 2008):

$$227 \quad EA = E_{st} \cdot \left(\frac{\pi}{4} \cdot \Phi_{bar}^2 \right) + E_{binder} \cdot \left[\frac{\pi}{4} \cdot (\Phi_{hole}^2 - \Phi_{bar}^2) \right] \quad (3a)$$

$$228 \quad EJ = E_{st} \cdot \left(\frac{\pi}{64} \cdot \Phi_{bar}^4 \right) + E_{binder} \cdot \left[\frac{\pi}{64} (\Phi_{hole}^4 - \Phi_{bar}^4) \right] \quad (3b)$$

229 where:

230 Φ_{bar} is the bolt diameter;

231 E_{st} is the steel elastic modulus;

232 E_{binder} is the elastic modulus of the binder surrounding the steel bar in the hole.

233 In the case in which the elastic modulus of the rock is considerably higher than the elastic
234 modulus of the material that surrounds the steel bar (for example cement mortar), it is pos-
235 sible to assume the simplified hypothesis of non-deformable rock, which leads to the follow-
236 ing estimation of β_c (and therefore, of α) and of k (and therefore of β):

$$237 \quad \beta_c \cong \frac{1}{t_{binder}} \cdot \frac{E_{binder}}{2 \cdot (1 + \nu_{binder})} \quad (4a)$$

$$238 \quad k \cong \frac{E_{binder}}{t_{binder}} \quad (4b)$$

239 where:

240 t_{binder} is the thickness of the binder annulus surrounding the steel bar;

241 ν_{binder} is the Poisson coefficient of the binder (generally assumed equal to 0.15).

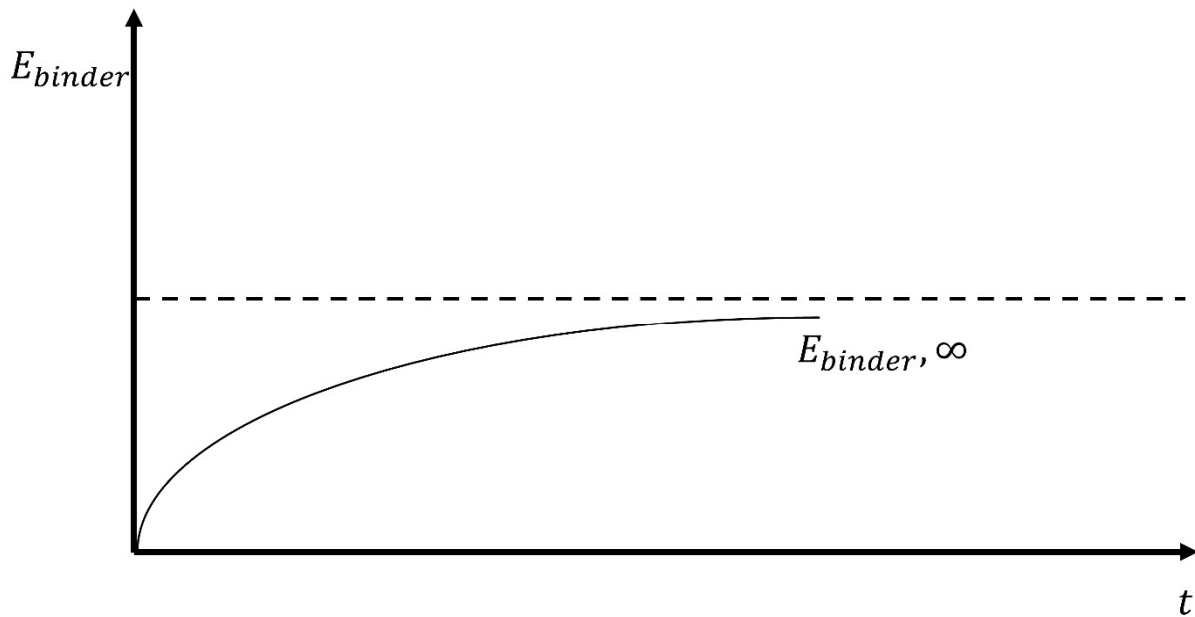
242 When using both cement grout or resin, the elastic modulus evolves over time from the
243 moment the material is injected into the hole. For resins, curing evolution over time is faster,
244 whereby setting occurs within few hours, while for cement grouts are more slowly, where
245 cement hydration is completed within several weeks (see Spagnoli 2018 for detailed infor-
246 mation). In both cases it is however possible to use the following negative exponential equa-
247 tion to estimate the trend of the elastic modulus over time (Fig. 3):

$$248 \quad E_{binder} \cong E_{binder, \infty} \cdot (1 - e^{-\varepsilon_E \cdot t}) \quad (5)$$

249 where:

250 $E_{binder, \infty}$ is the elastic modulus of the binder for a time t very large;

251 ε_E is a constant (having the inverse dimension of time) indicating the rate with which the
252 elastic modulus evolves from the initial null value to the asymptotic value $E_{binder, \infty}$. The
253 constant ε_E can be evaluated by knowing one or more E_{binder} intermediate values associ-
254 ated with certain values of time t .



255

256 **Fig. 3 Sketch of the evolution over time of the elastic modulus of the binder according**
257 **to the simplified trend of the negative exponential law.**

258 By estimating the time t at which the dislocation of the block occurs and, therefore, the
259 loading of the bolts, it is possible to determine from the equation 5 the value of the elastic
260 modulus E_{binder} to be used in the calculations (equations 3 and 4) for the analysis of passive
261 bolts used in the stabilization of rock blocks.

262 **Results and discussion**

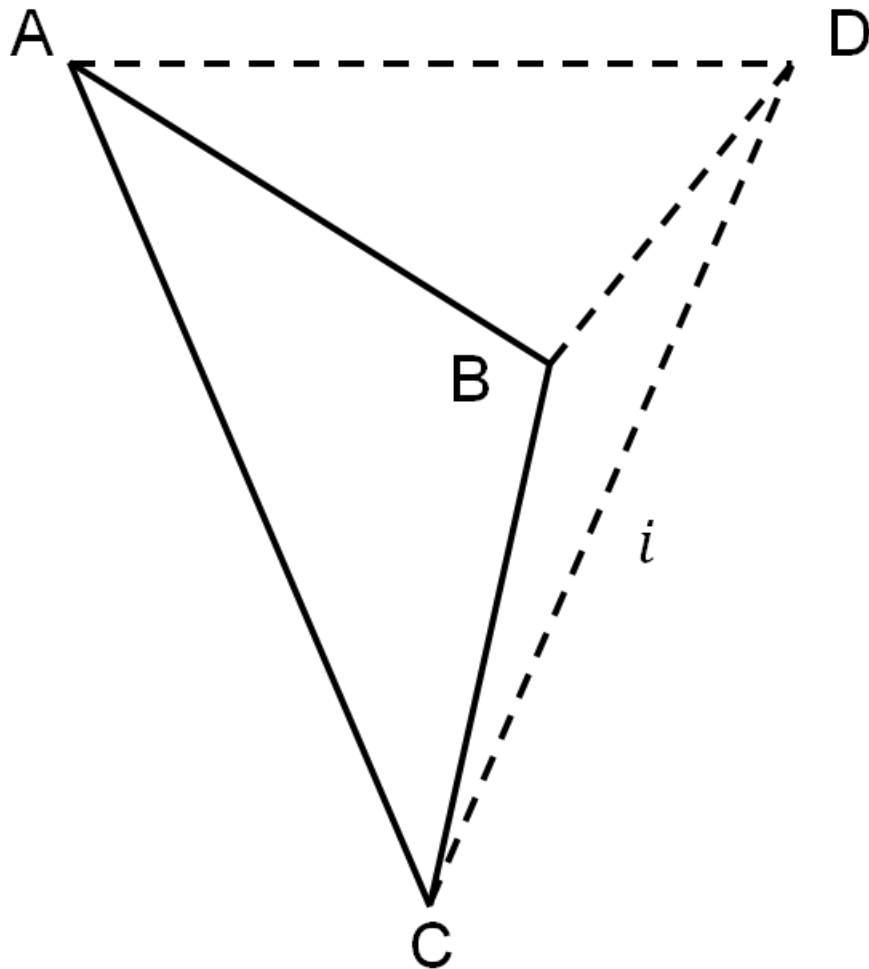
263 To study in detail the role of the mechanical properties of the binder used to connect a steel
264 bar of a fully encapsulated passive bolt to the surrounding rock, a parametric analysis of 729

265 cases has been developed by varying six fundamental parameters of the calculation, i.e. 3^6

266 cases:

- 267 1. The diameter of the steel bar ($\Phi_{bar} = 18\text{mm}, 27\text{mm}, 36\text{mm}$);
- 268 2. The thickness of the binder ring around the bar ($t_{binder} = 8\text{mm}, 12\text{mm}, 16\text{mm}$);
- 269 3. The length of the bolt in the unstable block ($L_a = 1\text{m}, 2\text{m}, 3\text{m}$);
- 270 4. The total length of the bolt ($L_{tot} = L_a + L_p = 4\text{m}, 5\text{m}, 6\text{m}$);
- 271 5. The elastic modulus of the binder ($E_{binder} = 4\text{GPa}, 8\text{GPa}, 12\text{GPa}$);
- 272 6. The displacement of the block with respect to the horizontal plane ($\gamma_{displ} = 30^\circ, 45^\circ,$
- 273 60°).

274 The first four parameters concern the geometry of the bolt (the characteristics of its cross section
275 and those related to the longitudinal development, with reference to the crossed rock block); the fifth
276 is the parameter related to the stiffness of the binder; finally, the last one concerns the **angle** of the
277 vector-displacement of the block, coinciding with the intersection line of its two sliding planes (Figure
278 4). **A, B and C are the vertices of the block on the vertical rock face; D: vertex inside the rock mass;**
279 ***i*: intersecting line of the sliding surfaces, coinciding with the direction of the block displacement**
280 **vector.** It has to be pointed out that normally annulus values of 16mm are not used, but it was dis-
281 cussed in the analysis to show the impact on the axial and shear forces obtained with the model.
282 **Besides, the model is also applicable for length values larger than those presented above (for in-**
283 **stance for cable bolts).**



284

285 **Fig. 4 Sketch of the pyramidal block considered in the calculations.**

286 The BRP calculation procedure was used to study the behavior of the bolts. Some simplify-
287 ing hypotheses are the basis of the study:

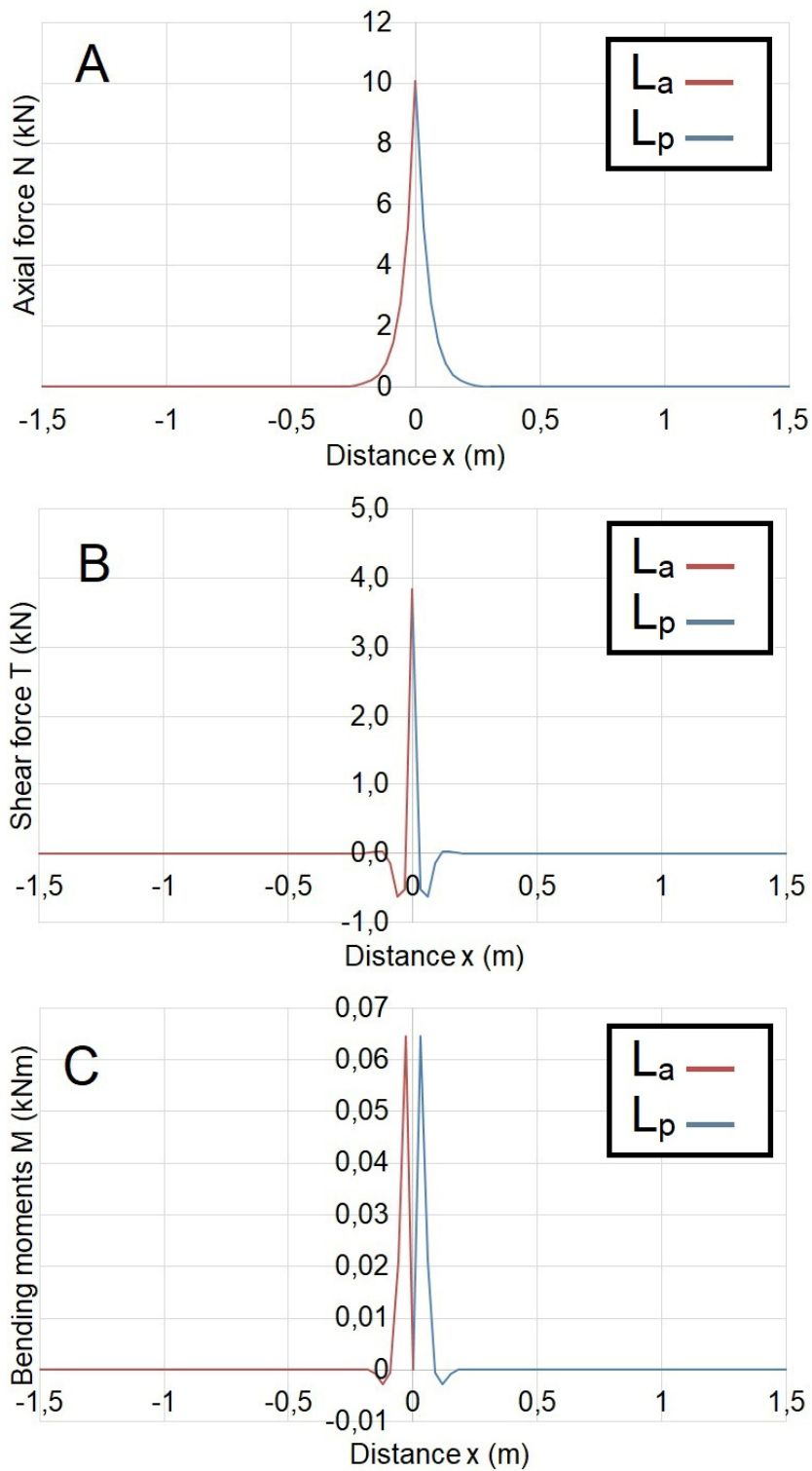
- 288 a. The potentially unstable rock block is pyramidal and is positioned on a vertical wall;
289 appears to be symmetrical with respect to the vertical plane passing through its inner
290 vertex D (Figure 4) and perpendicular to the rock face;
- 291 b. The block moves with a simple translation in the direction of the intersection line i ;
- 292 c. The bolt is a single element, horizontal and perpendicular to the rock face;
- 293 d. The bolt has a linear and elastic behavior, dictated by normal stiffness (EA) and by
294 flexural stiffness (EJ);

- 295 e. The interaction of the bolt with the surrounding rock is analyzed through linear and
296 elastic Winkler springs, both in the direction transverse to the bolt, and in the axial
297 direction;
- 298 f. The stiffness of the rock is considerably larger than the stiffness of the binder; for this
299 reason, the rock is considered infinitely rigid and does not influence the interaction
300 parameters α and β .

301 The other parameters necessary for the calculation were arbitrary considered constant in
302 the parametric study and they are:

- 303 • Poisson ratio of the binder ($\nu_{binder} = 0.15$);
- 304 • Elastic modulus of steel ($E_{st} = 210\text{GPa}$);
- 305 • Steel yield stress ($\sigma_{yield} = 400\text{MPa}$);
- 306 • Limit shear stress at the bolt-rock interface ($\tau_{lim} = 2\text{MPa}$);
- 307 • Local safety factors of the bolt, against the failure of the steel bar or failure of the bolt-
308 rock interface ($FS_{,bar} = 1.25$; $FS_{,pullout} = 1.25$).

309 The forces distribution along the bolt N, M and T for $L_a=3\text{m}$, $L_{tot}=6\text{m}$, $E_{binder}= 8\text{GPa}$,
310 $\gamma_{displ}=60^\circ$, $\Phi_{bar}= 27\text{mm}$ and $t_{binder} = 8\text{mm}$ is shown in Fig. 5. The origin of the distance axis
311 on Fig. 5 is positioned on the intersection with the sliding surface of the block. Because of
312 the flat trend of the lines at a certain distance from the origin, the graph has been cut. The
313 study allowed to derive the values of N_0 and T_0 that the bolt applies to the potentially unstable
314 rock block, in each of the 729 cases examined. In each graph obtained, the results of 27
315 analyzes are summarized. In particular, in these graphs, the values N_0 and T_0 are plotted
316 with varying the elastic modulus of the binder.



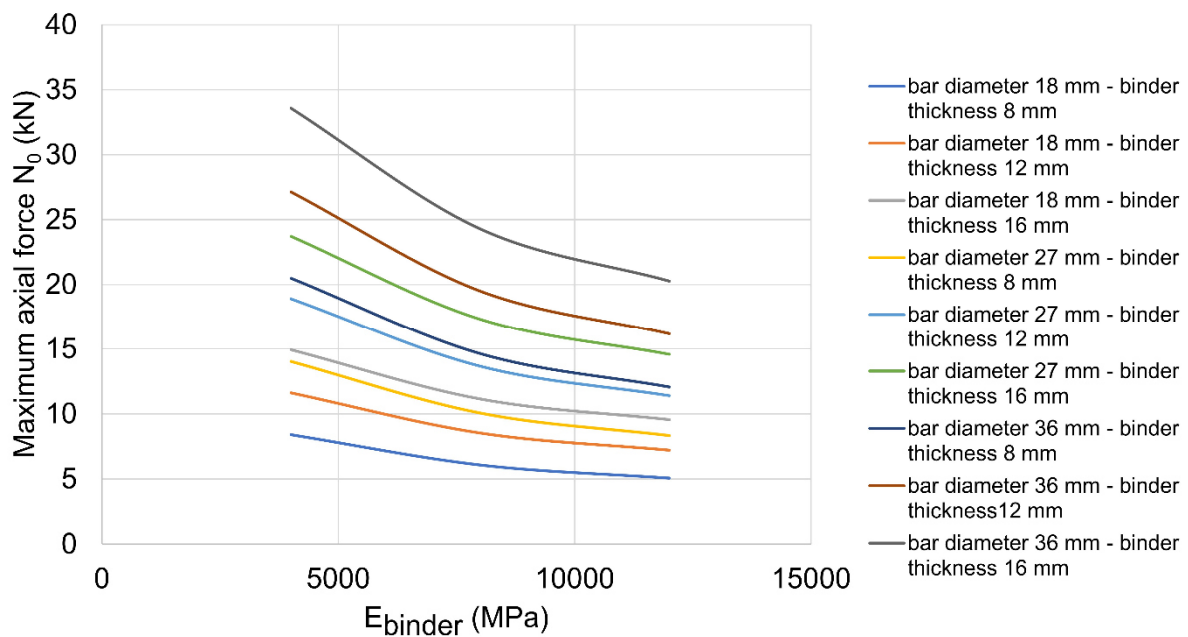
317

318 **Fig. 5. Trend of the axial force N (A), shear force T (B) and moment M (C) for a bolt**
 319 **with $L_a=3\text{m}$, $L_{tot}=6\text{m}$, $E_{binder}=8\text{GPa}$, $\gamma_{displ}=60^\circ$, $\Phi_{bar}=27\text{mm}$ and $t_{binder}=8\text{mm}$.**

320 From the analysis of the figures it is possible to see how the maximum axial tensile force N_0
 321 increases, as well as increasing the diameter of the bar, and:

- 322 • N_0 decreases as the elastic modulus of the binder increases;
- 323 • N_0 increases as the thickness of the binder annulus increases;
- 324 • N_0 is independent of the inclination with respect to the horizontal of the block dis-
- 325 placement vector.

326 Furthermore, there is no influence of the length L_a and the length L_{tot} on the value of N_0 ,
 327 when the values of the lengths in the unstable zone and in the stable rock are greater than
 328 or equal to 1 m. For this reason, the graphs that refer to the case of $L_a = 2\text{m}$ and $L_{tot} = 4\text{m}$
 329 (Figure 6) can also be considered representative of the other 8 L_a - L_{tot} combinations.



330

331 **Fig. 6. Trend of the axial tensile force N_0 with variation of the elastic modulus of the**
 332 **binder, the diameter of the steel bar, the thickness of the binder for the displacement**
 333 **vector angle, γ_{displ} , of 30° .**

334 From the analysis of the graphs of Figure 6 it can be seen how the characteristics of the
 335 binder (elastic modulus and thickness) have a great influence on the axial force N_0 . In fact,
 336 this force can even increase by 250% depending on the thickness of the grout and its elastic

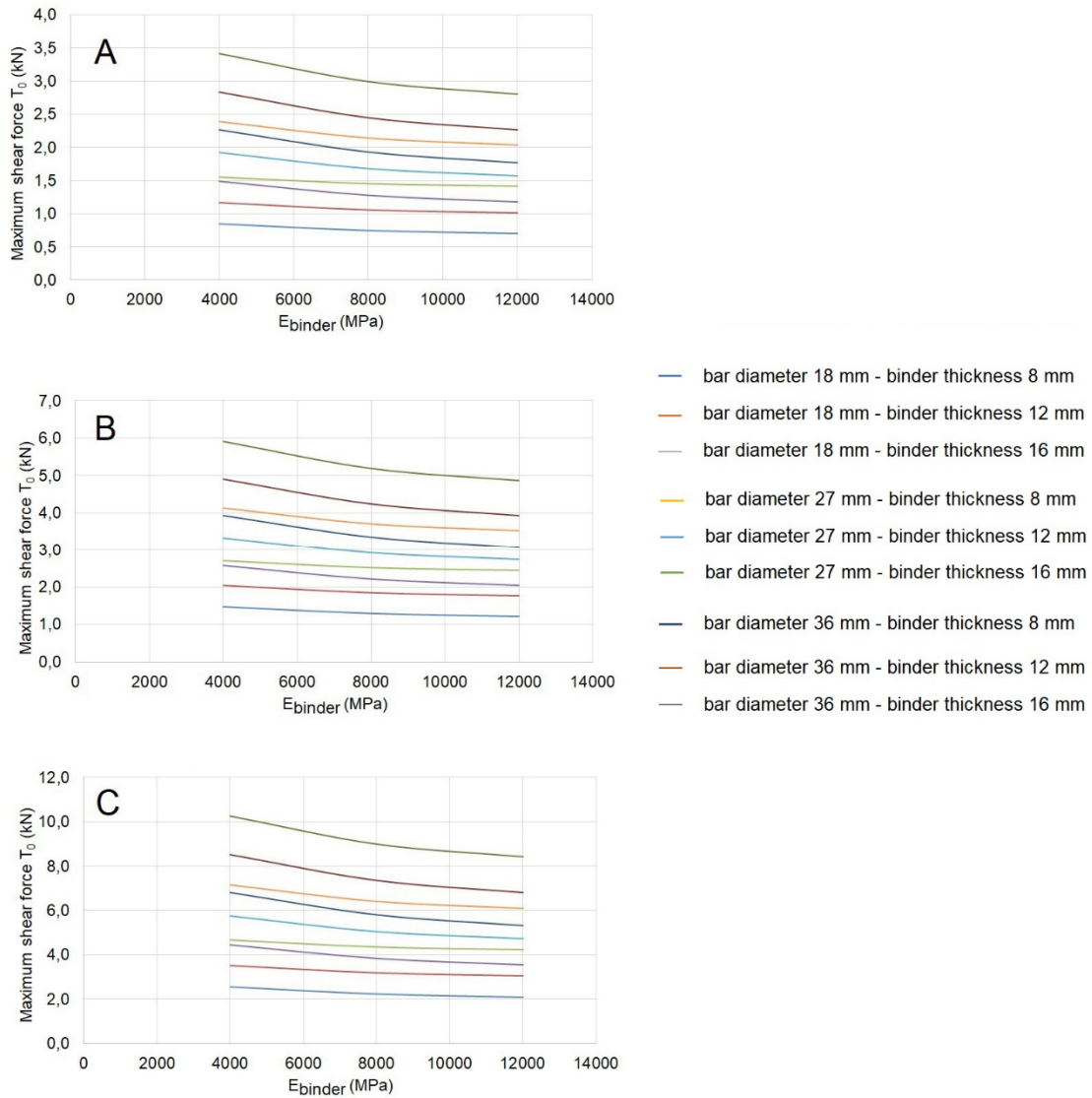
337 modulus. It is also possible to observe that the values of N_0 tend to increase for increasing
338 annulus grout thickness (from 8 to 16mm).

339 As for the maximum shear force T_0 value, it increases with the diameter of the bar, but also:

- 340 • It decreases with the increase of the elastic modulus of the binder (in a non-linear
341 way);
- 342 • It increases as the thickness of the grout annulus increases;
- 343 • It increases as the inclination of the vector-displacement of the block increases.

344 Also for T_0 there is no influence of length L_a and length L_{tot} . The three graphs that refer to
345 the case of $L_a = 2$ m and $L_{tot} = 4$ m (Figure 7) can, therefore, be considered representative
346 for all the values L_a and L_{tot} , provided they have a value greater than 1m.

347 For bar diameters of 18mm and with relatively small grout thicknesses (8 mm), the value of
348 T_0 remains negligible for any E_{binder} value. When the bar has high diameters and the thick-
349 ness of the grout is considerable (16mm), on the other hand, T_0 can vary with the elastic
350 modulus of the binder.



351

352 **Fig. 7. Trend of the shear force T_0 with variation of the elastic modulus of the binder,**
 353 **the diameter of the steel bar, the thickness of the binder, for three different values of**
 354 **the angle of the displacement vector γ_{displ} : 30° (A), 45° (B), 60° (C) for $L_a = 2m$ and L_{tot}**
 355 **= 4m.**

356 **Conclusions**

357 Passive rock bolting is a rock reinforcement system widely used both above ground and in
 358 the underground excavations. Its functioning mechanism is complex, as its loading and,
 359 therefore, the stabilizing effects are activated with the movement of the rock.

360 In the present work we tried to evaluate the effects of the mechanical and geometric char-
361 acteristics of the grout on the behavior of the bolt. The cementitious (or resinous) binder
362 used to connect the steel bolt bar to the rock, in fact, play a fundamental role also in the
363 development of the stabilizing forces that the bolt transmits to the potentially unstable rock
364 blocks.

365 For this purpose, an extensive parametric analysis was performed, varying some fundamen-
366 tal parameters of the fully encapsulated passive bolts. The calculation method used is the
367 BRP (Oreste and Cravero 2008; Oreste 2009), which allows to analyze in detail the behavior
368 of fully encapsulated passive bolts in the stabilization of blocks that tend to move on a rock
369 face. In the parametric analysis the geometric and mechanical parameters representing the
370 grout around the steel bar and, more precisely, the thickness and the elastic modulus of the
371 binder, were changed.

372 Furthermore, different values of the total length of the bolt and of its crossing length in the
373 block, the diameter of the steel bar and of the inclination of the vector-displacement of the
374 block with respect to the horizontal plane were considered. 729 different analyzes were de-
375 veloped to represent the typical cases that can be encountered in practice. From the results
376 of the calculation it was possible to detect how the stabilizing forces that the bolt applies to
377 the potentially unstable block depend markedly on the elastic modulus and on the thickness
378 of the binder itself on the edge of the steel bar. In particular, the axial force and the trans-
379 versal force applied by the bolt to the block decrease as the elastic modulus of the binder
380 increases and they increase as the binder thickness increases. Ultimately, it has been pos-
381 sible to observe a fundamental role of the binder on the behavior of the bolt and on its
382 effectiveness in the stabilization of the potentially unstable blocks on the rock walls. The
383 definition of the characteristics of the grout must be implemented not only in relation to ex-
384 ecution problems (speed up of the bolts installation, simplification of the execution phases,
385 guarantees of the final product), but also in relation to the efficiency of the bolting in the

386 stabilization of rock blocks, by achieving high values of stabilization forces. From the para-
387 metric analysis performed in this research, larger bolt and larger annulus thickness values
388 provided better results in terms of axial and shear forces, however it is recommended that
389 the mechanical properties (i.e. compressive strength and elastic module) of the pure grout
390 are not overperforming as it seems that larger values have a negative impact on N_0 and T_0 .

391 **Conflict of interests**

392 Authors declare they have no conflict of interest.

393 **References**

- 394 1. Bawden, F.W. (2011). Ground Control Using Cable and Rock Bolting. In: Darling, P.,
395 Ed., SME Mining Engineering Handbook, Society for Mining, Metallurgy and Explo-
396 ration Inc., Littleton, 616-617.
- 397 2. Carranza-Torres, C. (2009). Analytical and numerical study of the mechanics of rock-
398 bolt reinforcement around tunnels in rock masses. *Rock Mechanics and Rock Engi-
399 neering*, 42: 175–228, DOI 10.1007/s00603-009-0178-2.
- 400 3. Chappell, B.A., 1989. Rock bolts and shear stiffness in jointed rock mass. *J. Geotech.
401 Eng.* 115, 2, 179-197, [https://doi.org/10.1061/\(ASCE\)0733-9410\(1989\)115:2\(179\)](https://doi.org/10.1061/(ASCE)0733-9410(1989)115:2(179)).
- 402 4. Chen, S.H., Qiang, S., and Chen, S.F., Egger, P. 2004. Composite element model of
403 the fully grouted rock bolt. *Rock mechanics and Rock Engineering*, 37 (3), 193--212.
- 404 5. Henning P, Ferreira P (2010). In-stope bolting for a safer working environment. *Jour-
405 nal of the Southern African Institute of Mining and Metallurgy*, 110, 1: 47-51.
- 406 6. Indraratna, B., Kaiser, P.K., 1990. Design for grouted rock bolts based on the con-
407 vergence control method. *Int. J. Rock Mech. Min. Sci. Geomech. Abstr.* 27, 269–281.
- 408 7. Lancellotta, R., and Cavalera, J. (1999) *Fondazioni*. Mc Graw Hill, Milano

- 409 8. Lang TA (1961) Theory and practice of rock bolting. Trans Soc Min Engrs Am Inst
410 Min Metall Petrolm Engrs 220: 333–348.
- 411 9. Li, Y., Zhou, H., Zhang, L., Zhu, W., Li, S. and Liu, J. (2016). Experimental and nu-
412 merical investigations on mechanical property and reinforcement effect of bolted
413 jointed rock mass. Construction and Building Materials 126, 843–856.
- 414 10. Littlejohn GS, Bruce DA (1977). Rock Anchors-State of the Art. Foundation Publica-
415 tions Ltd, Brentwood (UK).
- 416 11. Nie W., Zhao Z.Y., Ning Y.J., Guo W., 2014. Numerical Studies on Rockbolts Mech-
417 anism using 2D Discontinuous Deformation Analysis. Tunnelling and Underground
418 Space Technology, 41: 223-233.
- 419 12. Oreste P (2008). Distinct analysis of fully grouted bolts around a circular tunnel con-
420 sidering the congruence of displacements between the bar and the rock. International
421 Journal of Rock Mechanics and Mining Sciences, 45(7): 1052-1067,
422 <https://doi.org/10.1016/j.ijrmms.2007.11.003>.
- 423 13. Oreste, P.P., and Cravero, M. (2008). An analysis of the action of dowels on the
424 stabilization of rock blocks on underground excavation walls. Rock Mechanics and
425 Rock Engineering, 41(6), 835–868, DOI 10.1007/s00603-008-0162-2.
- 426 14. Oreste PP, Dias D (2012) Stabilisation of the excavation face in shallow tunnels using
427 fibreglass dowels. Rock Mechanics Rock Eng., 45(4): 499-517. DOI:
428 10.1007/s00603-012-0234-1
- 429 15. Oreste, P.P. (2009). Face stabilisation of shallow tunnels using fibreglass dowels.
430 Proceedings of the Institution of Civil Engineers-Geotechnical Engineering, 162 (2),
431 95–109, doi: 10.1680/geng.2009.162.2.95.

- 432 16. Oreste, P. (2013). Face stabilization of deep tunnels using longitudinal fibreglass
433 dowels. *International Journal of Rock Mechanics & Mining Sciences*, 58, 127–140.
- 434 17. Ranjbarnia M, Fahimifar A, Oreste P (2014) A simplified model to study the behavior
435 of pre-tensioned fully grouted bolts around tunnels and to analyze the more important
436 influencing parameters. *Journal of Mining Science*, 50 (3), 533–548,
437 <https://doi.org/10.1134/S1062739114030156>.
- 438 18. Ranjbarnia M, Fahimifar A, Oreste P (2016) Practical Method for the Design of Pre-
439 tensioned Fully Grouted Rockbolts in Tunnels. *Int J Geomech* 16(1):
440 [https://doi.org/10.1061/\(ASCE\)GM.1943-5622.0000464](https://doi.org/10.1061/(ASCE)GM.1943-5622.0000464).
- 441 19. Spagnoli G (2018) A review of soil improvement with non-conventional grouts.
442 *International Journal of Geotechnical Engineering*,
443 <https://doi.org/10.1080/19386362.2018.1484603> (in press).
- 444

445 **FIGURE CAPTION**

446 **Fig. 1** Picture a fully encapsulated rock bolt

447 **Fig. 2** Schematic representation (not to scale) of the potentially unstable rock block
448 and of the passive bolt passing through it.

449 **Fig. 3** Sketch of the evolution over time of the elastic modulus of the binder according
450 to the simplified trend of the negative exponential law.

451 **Fig. 4** Sketch of the pyramidal block considered in the calculations.

452 **Fig. 5.** Trend of the axial force N (A), shear force T (B) and moment M (C) for a bolt
453 with $L_a=3\text{m}$, $L_{tot}=6\text{m}$, $E_{binder}=8\text{GPa}$, $\gamma_{displ}=60^\circ$, $\Phi_{bar}=27\text{mm}$ and $t_{binder}=8\text{mm}$.

454 **Fig. 6.** Trend of the axial tensile stress N_0 with variation of the elastic modulus of the
455 binder, the diameter of the steel bar, the thickness of the binder for the displacement
456 vector **angle**, γ_{displ} , of 30° .

457 **Fig. 7.** Trend of the shear force T_0 with variation of the elastic modulus of the binder,
458 the diameter of the steel bar, the thickness of the binder, for three different values of
459 the **angle** of the displacement vector γ_{displ} : 30° (A), 45° (B), 60° (C) for $L_a = 2\text{m}$ and L_{tot}
460 $= 4\text{m}$.

461